Anisotropy of cell wall polymers in branches of hardwood and softwood: A polarized FTIR study

ARTICLE *in* CELLULOSE · APRIL 2011

Impact Factor: 3.57 · DOI: 10.1007/s10570-011-9584-1

Cellulose (2011) 18:1433–1440
DOI 10.1007/s10570-011-9584-1

Anisotropy of cell wall polymers in branches of hardwood and softwood: a polarized FTIR study

Jasna Simonović · Jasna Stevanic · Daniela Djikanović · Lennart Salmén · Ksenija Radotić

Received: 11 March 2011 / Accepted: 13 August 2011 / Published online: 23 August 2011

Abstract The mechanical and physical properties of wood fibres are dependent on the organisation of their constituent polymers (cellulose, hemicellulose and lignin). Fourier Transform Infrared (FTIR) microscopy was used to examine the anisotropy of the main wood polymers in isolated cell wall fragments from branches of maple and Serbian spruce. Polarised FTIR measurements indicated an anisotropy, i.e. orientation of the cellulose microfibrils that was more or less parallel to the longitudinal axis of the cell wall. The hemicelluloses, glucomannan and xylan appeared to have a close link to the orientation of the cellulose and, thus, an orientation more parallel to the axis of the cell wall. An important result is that, in both maple and spruce samples, lignin was found to be organised in a parallel way in relation to the longitudinal cell wall axis, as well as to the cellulose. The results show that, despite the different lignin precursors and the different types of hemicelluloses in these two kinds of wood, lignin has a similar orientation, when it comes to the longitudinal axis of the cell wall.

Keywords Cellulose · Glucomannan · Lignin · Orientation · Wood · Xylan

Electronic supplementary material The online version of this article (doi:10.1007/s10570-011-9584-1) contains supplementary material, which is available to authorized users.

J. Simonović · D. Djikanović · K. Radotić (✉)
Institute for Multidisciplinary Research, Kneza Višeslava 1, 11000 Belgrade, Serbia
e-mail: xenia@imsi.rs

J. Stevanic · L. Salmén (✉)
Innventia, Box 5604, 114 86 Stockholm, Sweden
e-mail: lennart.salmen@innventia.com

Introduction

A wood fibre cell wall (CW) can be considered as a nano-composite, in which cellulose, lignin and hemicelluloses (xylan and glucomannan) are interconnected in an intricate manner, being regulated by the mechanism of the deposition of the main wood polymers during cell wall formation. It is well recognised that the cell wall development of cell wall expansion and deposition implies an anisotropic arrangement of the cell wall components (Baskin 2005). The cell wall consists of several layers, i.e. the outermost primary wall (P), the outer secondary wall (S_1), the middle secondary wall (S_2) and the inner secondary wall (S_3). Due to its relatively larger thickness in relation to the other cell wall layers (80% by weight), the properties of the S_2 layer dominate the properties of the cell wall. Cellulose is a straight chain polymer that adopts an extended and rather stiff rod-like conformation (Salmon and Hudson 1997). It gives mechanical strength to the CWs, due to its relatively parallel orientation to the longitudinal axis of the CW (Marchessault 1962; Åkerholm and

Salmén 2001). The main difference among the hemicelluloses of hardwood and softwood exists in the content of the xylan and glucomannan, with a greater content of xylan in hardwood and a greater content of glucomannan in softwood (Aspinall 1980). Softwood xylans also differ from hardwood xylans in their lack of acetyl groups (Liang et al. 1960). Spectroscopic and microscopic studies of lignin indicate that the polymer has an ordered structural organisation (Atalla and Agarwal 1985; Radotic et al. 1994; Micic et al. 2000). There is also a difference in lignin monomeric precursors between the CWs of these two wood groups; the lignin in softwood contains guaiacyl monomers and the lignin in hardwood contains both guaiacyl and syringyl monomers (Sarkanen and Hergert 1971). Although, it is known that, in the CW framework, the cellulose microfibrils are tightly embedded in the matrix of lignin and hemicellulose the assembly of these components in the cell wall and its structural organisation is not being sufficiently understood. Understanding the arrangement and anisotropy of the polymers in the CW is important for understanding the mechanical properties of wood, which has implications in plant response to stress, but also in possible applications of wood as a source of new biomaterials.

Recently cell wall anisotropy has been studied by using differential polarization fluorescence imaging, a method which estimates linear dichroism of the cell walls by following orientation of congo red-stained cellulose (Steinbach et al. 2008). On the other hand, imaging FT-IR polarized microscopy has been shown to be a valuable tool in assessing the anisotropy, i.e. orientation of cell wall polymers in the structure of fibres (Stevanic and Salmén 2009). The orientation of cellulose, glucomannan, xylan and lignin, as essential components of wood, can thus be analysed in relation to the axis of the fibre. According to literary data, lignin orientation in the cell wall has not been clearly resolved. It is a branched polymer, mostly assumed to have an isotropic (unordered) organisation in the cell wall (Monties 1998; Hatfield and Vermeris 2001). The FT-IR polarized microscopy was used here to compare the orientation distribution of the wood polymers in cell wall fibres from branches of a hardwood, viz. maple (*A. platanoides*) and a softwood, viz. Serbian spruce [*P. omorika* (Panč) *Purkyne*]. Serbian spruce was a major subject of our previous studies, in which data was obtained on the enzymic antioxidative system and the related structural characteristics of the cell wall in the *P. omorika* needles (Bogdanovic et al. 2006), as well as on the effect of seasonal changes on the antioxidant enzymes in the natural habitat of the species (Bogdanovic et al. 2007). Since Serbian spruce is a protected species, we chose branches as the subject of our study.

Branches have a similar structure to that of the trunk of a tree. However, they are affected in different ways by gravitational loads. This leads to the production of higher or lower amounts of reaction wood; in softwood, this concerns compression wood in the lower part of the branch and, in hardwood, it concerns tension wood in the upper part of the branch. The opposite wood, on the opposite side of the branch, has a similar structure to that of the trunk wood. In the present study, straight branches were analysed that did not show the anatomical characteristics of the formation of reaction wood.

Experimental

Cell wall isolation

Cell wall materials were obtained from branches of maple (*A. platanoides*) and Serbian spruce [*P. omorika* (Panč) *Purkyne*]. The branches were taken at a height of 2 m above ground level from trees of similar ages (50–60 years old). The middle part of a straight branch at a point 1 m away from the trunk was used. Samples were taken from the outermost annual rings of a branch, starting at point M on a cross section, as illustrated in Fig. 1. At this point, it may be considered that the branch is composed of mature wood, while it may be considered that the very inner rings consist of juvenile wood. At this position, being mature wood, the variation of the cellulose microfibril orientation is small between annual rings. The shape of the cross section of the branch that was used was round, with rings that were almost concentric, indicating that there were insignificant levels of reaction wood in the samples used. The absence of tension wood was verified by the ratio of the 1,051–1,034 cm^{-1} peaks in the absorption FTIR spectra obtained from the maple fibres. The bands at 1,034 and 1,051 cm^{-1} have been assigned to the C–O stretching of the glycosidic link (Marchessault 1962). This ratio is similar to the ratio of the same peaks in the FTIR spectra of normal poplar

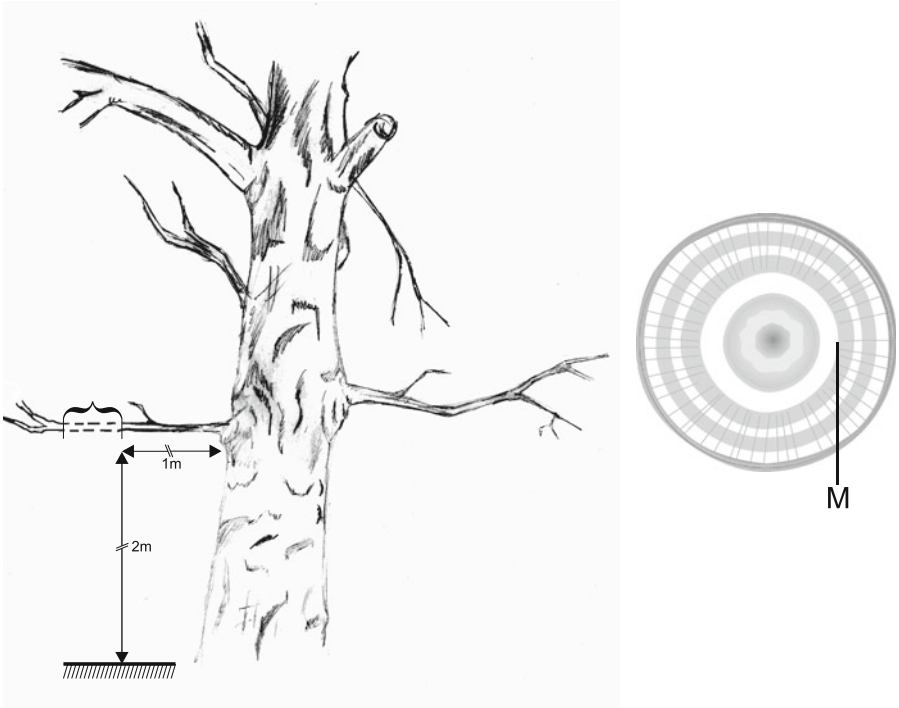

Fig. 1 *Left* A schematic presentation, showing the position of the branch on the tree and its height above ground, as well as the part of the branch chosen for sample collection. *Right* A sketch of the cross section of the branch is shown. The outermost annual rings of the branch, starting from M, were used in the experiments

wood obtained by Gierlinger et al. (2008), where the FTIR spectra of normal and tension wood were compared. In the FTIR spectra of tension wood, there was a shift of the 1,051–1,060 cm^{-1} and a drastic increase in the 1,060 cm^{-1} in relation to the 1,034 cm^{-1} band. The 1,060 cm^{-1} has been assigned to the C–O stretching (C-3–O-3) (Marchessault 1962; Gierlinger et al. 2008).

After removing the bark, the wood from the outermost annual rings were sliced into sticks.

To obtain extractive free cell walls, 1 g of wood was homogenized in 10 mL of 80% methanol in 50 mL Big Clean tubes filled with a stainless steel matrix for 45 s at a speed of 4.5 m/s, using a FastPrep-24 apparatus (MP Biomedicals, Santa Ana, CA, USA). After stirring for 5 min at room temperature, the sample was again subjected to FastPrep homogenization at the same speed, which is a preferred technique in the case of wood material (Melton and Smith 2001). The homogenate was stirred at room temperature for 1 h and centrifuged at 1,500×*g* for 5 min. Low-speed centrifugation is a preferred technique, when the amounts of tissue are small (Melton and Smith 2001). The pellet obtained was re-extracted twice, using 10 mL of 80% methanol (Harris 1983; Chen et al. 2000). In order to remove the extractives, the pellet that had been obtained was then subjected to washing steps, according to Strack et al. (1988) and Chen et al. (2000): 1× (1 M NaCl, 0.5% of Triton X-100), 2× distilled water, 2× 100% methanol, 2× 100% acetone. In each washing step, the sample was homogenized in 20 mL of corresponding washing solution and then subsequently stirred for 10 min at room temperature. After each washing step, the homogenate was centrifuged at 1,500×*g* for 10 min. The supernatant was subsequently removed. These isolation and purification processes enable the obtaining of pure cell wall fragments, with the polymers structure preserved (Harris 1983; Chen et al. 2000), as shown in Fig. 2. Prolonged beating may, for chemical pulps where a considerable part of the cell wall material has been removed, give rise to a decreased microfibril angle of the cellulose microfibrils. As the studied fibres here were in their native form the more rigid structure is believed to have prevented such reorientations to occur. The CW was dried at 60 °C for 1 h.

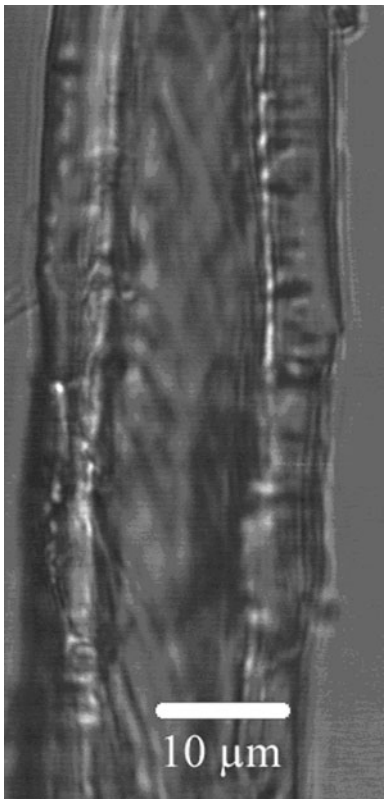

Fig. 2 An isolated cell wall fragment from a Serbian spruce branch fibre, i.e. tracheid. The intact cell wall structure is clearly seen. The image was obtained by using a Carl Zeiss LSM 410 Microscope, in transmission mode, Zoom 2, Lens 5, and Magnification 100 × 1.3

FTIR microscopy

FTIR microscopy measurements were carried out using a Spectrum Spotlight 400 FTIR Imaging System (Perkin Elmer Inc, Shelton, CT, USA). The area of interest was first displayed, using a visible CCD camera to locate the cell wall area, which was then irradiated using mid-IR light. The scanning was carried out in imaging mode using an array detector, providing a pixel resolution of 6.25 µm × 6.25 µm, a spectral resolution of 4 cm^{-1} and a spectral range from 1,800 to 720 cm^{-1}.

The CW fragments were mounted on a sample stage, as parallel as possible to the orientation of the 0° polarisation. For each tree species, several samples were observed under the optical microscope, and one well aligned sample was chosen as a representative sample which was subjected to the measurement. The incident IR radiation was polarised by a gold wire grid polariser, with 0–90° polarisation in relation to the fibre orientation, at intervals of 5°. The IR spectra obtained were processed by the following software: Spotlight 1.5.1, HyperView 3.2 and Spectrum 6.2.0 (Perkin Elmer Inc., Shelton, CT, USA). In order to minimise the effects of CO_2 and H_2O, the spectra were corrected by applying an atmospheric correction function. An automatic baseline correction function was used to remove the slope. A baseline offset correction function was also applied, so that all the spectra were adjusted to a uniform baseline.

The absorbance spectra recorded at polarisation modes of 0 and 90° were processed, using the following equation, yielding the linear dichroism spectrum, characteristic of orientation and anisotropic organization of the absorbance dipoles:

$$R = A_{0^\circ} - A_{90^\circ}$$

where R is the anisotropy spectra, indicating the orientation of components, A_{0° is the absorbance spectra recorded at 0° and A_{90° is the absorbance spectra recorded at 90°. An average orientation spectrum was calculated for both samples, based on fifteen individual spectra selected from each sample.

For an in-depth study of the polymer orientation, three areas were selected from each sample. The relative absorbance spectra were calculated in the same way for each sample and presented as relative absorption peaks according to the following:

$$RA = \left(\frac{I_P - I_{min}}{I_{max} - I_{min}}\right)$$

where RA is the relative absorbance, I_P is the intensity of the absorbed IR radiation at a given angle of the polarisation (P), I_{max} is the maximal intensity observed for a given vibration and I_{min} is the minimal intensity observed the same vibration. These relative absorbance values were presented in relation to the angle of the incident IR polarisation from 0 to 90° (Stevanic and Salmén 2009).

Results and discussion

Figure 3 presents the average orientation, anisotropy, spectra for the cell wall samples from maple to Serbian spruce. Due to the IR absorption in the wavenumber interval between 900 and 1,100 cm^{-1} being too high, this area has been masked off in the

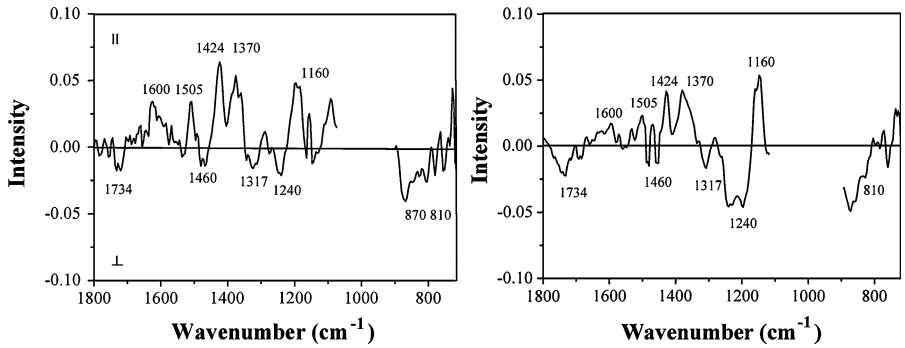

Fig. 3 The average orientation spectra of Serbian spruce (*left*) and maple (*right*). Absorption peaks, characteristic for different wood polymers, are indicated in each spectrum; cellulose—1,160, 1,317, 1,370 and 1,424 cm^{-1}; xylan—1,240, 1,460 and 1,734; glucomannan—810 and 870 cm^{-1}; lignin—1,505 and 1,600 cm^{-1}

figure. Spectral signals, related to absorbances from the cellulose, hemicellulose (glucomannan and xylan) and lignin in the wavenumber range between 1,800 and 720 cm^{-1}, can be identified. Positive signals indicate that their corresponding functional groups are arranged in a more parallel orientation to the fibre axis, while negative signals indicate that the corresponding functional groups are arranged in a more perpendicular orientation to the longitudinal CW axis.

For both the spruce and maple samples, three distinct vibration bands that were related to cellulose, viz. the antisymetric C–O–C bridge stretching vibration at 1,160 cm^{-1}, the C–H bending vibration at 1,370 cm^{-1} and the C–OH bending vibration of the CH_2–OH group at 1,424 cm^{-1}, were found to be oriented parallel to the longitudinal axis (Liang et al. 1960; Marchessault 1962; Åkerholm et al. 2004). The intensities of these peaks were high and sharp. A cellulose vibration (CH_2 wagging vibration) at 1,317 cm^{-1} (Liang et al. 1960; Marchessault 1962; Åkerholm et al. 2004) was also visible, oriented perpendicularly to the cellulose chain.

For the xylan, both for the spruce and maple, a negative signal was observed from the carbonyl group vibration, the C=O stretching vibrations in the O=C–OH group of the glucuronic acid units at 1,734 cm^{-1} (Liang et al. 1960; Marchessault 1962; Åkerholm and Salmén 2001). Signals of the CH_2 symmetric bending on the xylose ring at 1,460 cm^{-1} and of the C–O stretching in the O=C–O group at 1,240 cm^{-1} (Liang et al. 1960; Marchessault 1962) also appeared in the negative field. The intensity of these bands was quite low. All of these xylan groups are oriented perpendicularly to the molecular axis. Due to this, the negative xylane vibrations mean that xylan has an orientation more parallel to the longitudinal axis of the cell wall.

A glucomannan absorbance vibration, indicating the orientation of glucomannan, was observed at 810 cm^{-1} (equatorially aligned hydrogen on the C_2 atom in the mannose residue) (Liang et al. 1960; Marchessault 1962; Åkerholm and Salmén 2001). The peak was negative for both spectra, i.e. for the maple and spruce samples. This group is oriented orthogonally to the glucomannan backbone, which is the reason why it may be concluded that glucomannan is also oriented in parallel to the CW longitudinal axis in branch fibres from both these trees. An orientated absorption vibration of glucomannan was also found at 870 cm^{-1} for the spruce CW, which may be due to the higher content of glucomannan in spruce, compared to maple. For spruce, such a clear orientation of glucomannan was previously reported, using FTIR microscopy (Stevanic and Salmén 2009).

Two characteristic vibrations were analysed for lignin. A lignin vibration (the C=C aromatic ring vibrations) at 1,505 cm^{-1} (Atalla and Agarwal 1985; Faix 1991) showed a positive orientation of the lignin structure in both samples. Furthermore, the lignin vibration (the C=C aromatic ring vibrations plus C=O stretch) at 1,600 cm^{-1} (Atalla and Agarwal 1985; Faix 1991) displayed a positive orientation of the lignin structure in both samples. Since these vibrations occur parallel to the aromatic ring structure, it may be deduced that there is an orientation of lignin parallel to the longitudinal CW axis.

Figures 4, 5 and 6 illustrate the dependence of the relative absorbance of different peaks, as a function

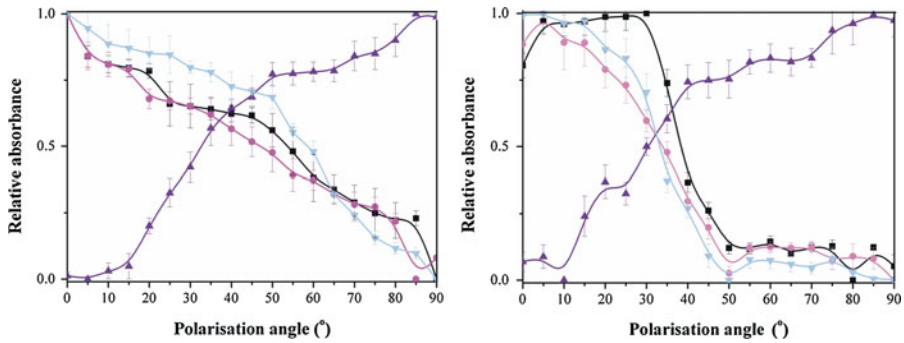

Fig. 4 The relative absorbance of IR characteristic absorption bands related to cellulose, plotted against the polarisation angle for spruce (*left*) and maple (*right*). (*Filled inverted triangle cyan*) C–O–C stretching at 1,160 cm^{-1}, (*filled triangle violet*) CH_2 wagging at 1,317 cm^{-1}, (*filled circle magenta*) C–H bending at 1,370 cm^{-1} and (*filled square black*) C–OH bending at 1,424 cm^{-1}

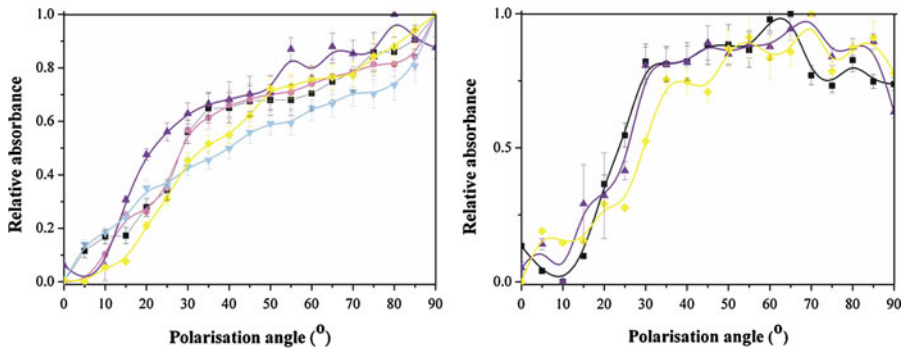

Fig. 5 The relative absorbance of IR characteristic absorption bands for hemicelluloses (xylan and glucomannan) plotted against the polarisation angle for spruce (*left*) and maple (*right*). Xylan: (*filled circle magenta*) C–O stretching at 1,240 cm^{-1}, (*filled diamond yellow*) CH_2 bending at 1,460 cm^{-1}, (*filled square black*) C=O stretching at 1,734 cm^{-1}; glucomannan: (*filled triangle violet*) equatorially aligned H vibration at 810 cm^{-1}, (*filled inverted triangle cyan*) 870 cm^{-1}

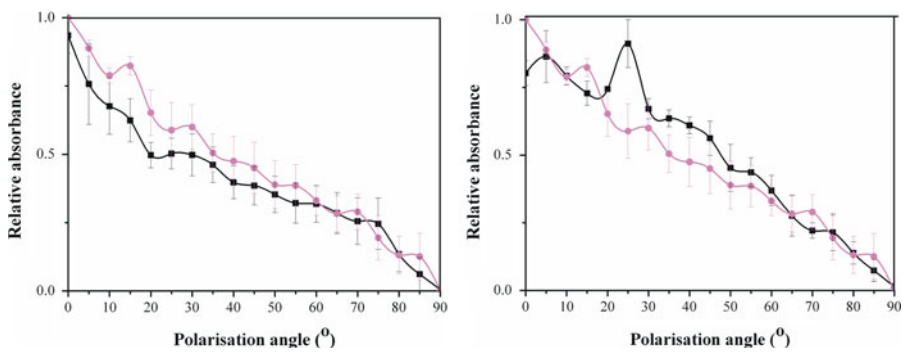

Fig. 6 The relative absorbance of IR characteristic absorption bands for lignin, plotted against the polarisation angle for spruce (*left*) and maple (*right*): (*filled square black*) C=C aromatic vibration at 1,505 cm^{-1}; (*filled circle magenta*) C=C aromatic vibration plus C=O stretch at 1,600 cm^{-1}

of the polarisation angle in the CW fragments from maple to spruce branches. For each polarisation angle, an average absorbance value was calculated from three original absorbance values for the chosen points. It is evident (Fig. 4) that the three cellulose peaks (1,160,1,370 and 1,424 cm^{-1}) had high

absorption levels at low polarisation angles, which is a consequence of a more parallel orientation of the corresponding groups to the CW longitudinal axis. The fourth cellulose peak (the perpendicular signal at 1,317 cm^{-1}) had the greatest intensity at a high polarisation angle, due to the perpendicular orientation of the corresponding group (Fig. 4). The orientation distribution for the two samples suggests that the cellulose is more uniformly arranged, parallel to the CW longitudinal axis in a maple sample, than it is in a corresponding spruce sample.

For the hemicelluloses, i.e. glucomannan and xylan, the characteristic band signals (1,240, 1,460, 1,734 and 810 cm^{-1}) increased with an increase in the polarisation angle, in the maple and spruce samples. Due to the parallel orientation of these side groups in xylan and glucomannan, respectively, an orientation parallel to the longitudinal CW axis is indicated for both hemicelluloses (Fig. 5). The high resemblance to the respective orientation of cellulose in the spruce and maple samples suggests a high degree of interaction between these carbohydrates during the formation of the CW.

For the lignin, the characteristic band signals (1,505 and 1,600 cm^{-1}) decreased with an increase in the polarisation angle (Fig. 6), indicating that lignin is organised in parallel with the longitudinal CW axis in both wood samples. Opposite to the fibrilar organisation of the cellulose macromolecules, lignin is mostly considered to have isotropic, unordered structure, being a branched polymer, with possibility of an enormous number of rearrangements within the monolayer, in such a way that they can form hydrogen and other non-covalent bonds (Micic et al. 2002). However, there have been Raman spectroscopy evidences (Atalla and Agarwal 1985) that the lignin aromatic rings may be oriented in parallel with a cell wall surface, as well as indications of lignin orientation along the stems of the young poplar trees, both in normal and tension wood (Olsson et al. 2011). The results in this study are strong evidence that in branches of both maple and spruce, lignin is oriented in parallel with the longitudinal cell wall axis. The lignin orientation in parallel with the cellulose fibres may be enabled by the strong non-covalent attractive interactions between phenyl rings and cellulose OH groups. Molecular dynamics calculations (Houtman and Atalla 1995) have shown that this type of interaction between model cellulose microfibrils and lignin model oligomers is sufficient to orient the phenyl rings, as well as the lignin oligomers parallel to the cellulose surface. Other studies have shown that cellulose acts as a templeting structure for lignin orientation during its synthesis (Micic et al. 2003). Lignin model compounds polymerised directly on a cellulose support arranged themselves as a self-assembled film spread over the cellulose, while the structure of lignin model compounds polymerised in a bulk solution and afterwards deposited on cellulose did not form such a layer (Micic et al. 2003).

Our results show that, in spite of different lignin precursors and different types of hemicelluloses in the two types of wood, lignin has a similar orientation with regard to the longitudinal CW axis. However, due to the more linear absorbance relation of the lignin peaks versus the polarisation angle, it may be deduced that the orientation distribution for the lignins does not seem to be so closely associated with the respective orientation of the carbohydrates in each cell wall sample (Figs. 4, 5 and 6). This may indicate a looser association of lignin with carbohydrates during cell wall formation.

It was earlier shown that various cell wall polymers contribute differently to the mechanical properties of the wall, in relation to the orientation of the whole cell wall (Bergander and Salmén 2002). The parallel orientation of cellulose with the longitudinal CW axis is important for the mechanical properties of the CW. This has been observed in experimental (Åkerholm and Salmén 2001) and model studies (Bergander and Salmén 2002), which showed that the elastic constants of cellulose almost exclusively determine the elastic properties in the longitudinal direction of the CW.

A parallel orientation of both lignin and hemicelluloses to the cellulose and longitudinal CW axis in maple and spruce branches indicate that the mechanical properties in the transverse direction of the CW is even more dependent on the orthogonal properties of the polymers than previously thought.

Conclusions

It has been demonstrated here that the hemicelluloses of both xylan and glucomannan are oriented in parallel to the cellulose and more or less parallel to

the axis of a cell wall, in isolated CW fragments from maple to spruce branch fibres. There was also a clear indication of lignin being orientated parallel to the longitudinal CW axis in both the maple and spruce branch fibres. However, the lignin orientation seems to not strictly follow the orientation of the carbohydrates, which is why it may be anticipated that there is a looser association of lignin to them.

Acknowledgments This work was supported by the Ministry of Science and Technology of the Republic of Serbia (Project #173017) and a Short Time Scientific Mission in COST Action FP0802 by Jasna Simonović at Innventia, Stockholm, Sweden. The Wallenberg Wood Science Center is acknowledged for funding of Jasna Stevanic and Lennart Salmén. We also acknowledge Gabor Stein and Krzysztof Pawlak, Biology Research Center, Szeged, Hungary, for obtaining images of the cell wall fragments.

References

Åkerholm M, Salmén L (2001) Interactions between wood polymers studied by dynamic FT-IR spectroscopy. Polymer 42:963–969

Åkerholm M, Hinterstoisser B, Salmén L (2004) Characterization of the crystalline structure of cellulose using static and dynamic FT-IR spectroscopy. Carbohydr Res 339:569–578

Aspinall GO (1980) Chemistry of cell wall polysaccharides. In: Priess J (ed) The biochemistry of plants: a comprehensive treatise. Academic Press, New York, pp 477–500

Atalla RH, Agarwal UP (1985) Raman microprobe evidence for lignin orientation in the cell walls of native woody tissue. Science 227:636–638

Baskin TI (2005) Anisotropic expansion of the plant cell wall. Annu Rev Cell Dev Biol 21:203–222

Bergander A, Salmén L (2002) Cell wall properties and their effects on the mechanical properties of fibres. J Mater Sci 37:151–156

Bogdanovic J, Djikanovic D, Maksimovic V, Tufegdzic S, Djokovic D, Isajev V, Radotic K (2006) Phenolics, lignin content and peroxidase activity in *Picea omorika* lines. Biol Plant 50:461–464

Bogdanovic J, Milosavic N, Prodanovic R, Ducic T, Radotic K (2007) Variability of antioxidant enzyme activity and isoenzyme profile in needles of Serbian spruce (*Picea omorika* (Panc.) Purkinye). Biochem System Ecol 35: 263–273

Chen M, Sommer AJ, McClure JW (2000) Fourier transform–IR determination of protein contamination in thioglycolic acid lignin from radish seedlings and improved methods for extractive-free cell wall preparation. Phytochem Anal 11:153–159

Faix O (1991) Classification of lignins from different botanical origins by FTIR spectroscopy. Holzforschung 45:21–27

Gierlinger N, Goswami L, Schmidt M, Burgert I, Coutand C, Rogge T, Schwanninger M (2008) In situ FT-IR microscopic study on enzymatic treatment of poplar wood cross-sections. Biomacromolecules 9:2194–2201

Harris PJ (1983) Cell walls. In: Hall JL, Moore AL (eds) Isolation of membranes and organelles from plant cells. Academic Press, London, pp 25–53

Hatfield R, Vermeris W (2001) Lignin formation in plants. The dilemma of linkage specificity. Plant Physiol 126:1351–1357

Houtman CJ, Atalla RH (1995) Cellulose: lignin interactions. A computational study. Plant Physiol 107:977–984

Liang CY, Basset KH, McGinnes EA, Marchessault RH (1960) Infrared spectra of crystalline polysaccharides; VII. Thin wood sections. Tappi 43:232–235

Marchessault RH (1962) Application of infra-red spectroscopy to cellulose and woody polysaccharides. Pure Appl Chem 5:107–129

Melton LD, Smith BG (2001) Current protocols in food analytical chemistry. Wiley, New York

Micic M, Jeremic M, Radotic K, Mavers M, Leblanc R (2000) Visualization of artificial lignin supramolecular structures. Scanning 22:288–294

Micic M, Orbulescu J, Radotic K, Jeremic M, Sui G, Zheng Yu, Leblanc RM (2002) ZL-DHP lignin model compound at the air–water interface. Biophys Chem 99:55–62

Micic M, Radotic K, Jeremic M, Leblanc RM (2003) Study of self-assembly of the lignin model compound on cellulose model substrate. Macromol Biosci 3:100–106

Monties B (1998) Novel structures and properties of lignins in relation to their natural and induced variability in ecotypes, mutants and transgenic plants. Polym Degrad Stabil 59:53–64

Olsson A-M, Bjurhager I, Gerber L, Sundberg B, Salmén L (2011) Ultra-structural organisation of cell wall polymers in normal- and tension wood of aspen revealed by polarisation FT-IR microscopy. Planta 233:1277–1286

Radotic K, Simic-Krstic J, Jeremic M, Trifunovic M (1994) A study of lignin formation at the molecular level by scanning tunneling microscopy. Biophys J 66:1763–1767

Salmon S, Hudson SM (1997) Crystal morphology, biosynthesis and physical assembly of cellulose chitin and chitosan. J Macromol Sci C37:199–263

Sarkanen KV, Hergert HL (1971) Classification and distribution. In: Sarkanen KV, Ludwig CH (eds) Lignins: occurrence, formation, structure and reactions. Wiley, New York, pp 43–94

Steinbach G, Pomozi I, Zsiros O, Páy A, Horváth GV, Garab G (2008) Imaging fluorescence detected linear dichroism of plant cell walls in laser scanning confocal microscope. Cytometry 73A:202–208

Stevanic J, Salmén L (2009) Orientation of the wood polymers in the cell wall of spruce wood fibres. Holzforschung 63:497–503

Strack D, Heilemann J, Wray V, Dirks H (1988) Cell wall: conjugated phenolics from coniferae leaves. Phytochemistry 28:2071–2078